Rafoxanide and Closantel inhibit SPAK and OSR1 kinases by binding to a highly conserved allosteric site on their *C*-terminal domains

Mubarak A. AlAmri,[a] Hachemi Kadri,[a] Luke J. Alderwick,[b] Nigel S. Simpkins,[c] Youcef Mehellou[d]*

[a] Mubarak A. AlAmri and Dr. Hachemi Kadri
School of Pharmacy
University of Birmingham
Edgbaston, Birmingham B15 2TT (UK)
[b] Dr. Luke J. Alderwick
Birmingham Drug Discovery Facility
School of Biosciences
University of Birmingham
Edgbaston, Birmingham B15 2TT (UK)
[c] Prof. Nigel S. Simpkins
School of Chemistry
University of Birmingham
Edgbaston, Birmingham B15 2TT (UK)
[d] Dr. Youcef Mehellou
School of Pharmacy and Pharmaceutical Sciences
Redwood Building, Cardiff University
Cardiff CF10 3NB (UK)
Tel: 0044 (0) 2920875821
Email: MehellouY1@cardiff.ac.uk

Supporting information for this article is given via a link at the end of the document.((Please delete this text if not appropriate))

Abstract: SPAK and OSR1 are two protein kinases that emerged as attractive targets in the discovery of novel antihypertensive agents due to their role in regulating electrolyte balance in vivo. In this work, we report on the identification of an allosteric pocket on their highly conserved *C*-terminal domains, which influences their kinase activity. Also, we show that some known WNK-signaling inhibitors bind to this allosteric site. Using in silico screening, we identified Rafoxanide, an anti-parasitic agent, as a novel allosteric inhibitor of SPAK and OSR1. Collectively, this work will facilitate the rational design of novel SPAK and OSR1 kinase inhibitors that could be useful antihypertensive agents.

Cellular cation-chloride co-transporters play important roles in maintaining electrolyte balance, a phenomenon that is critical to many physiological processes such as cell volume regulation and neuronal excitability.[1] Among the emerging signaling pathways involved in the in vivo regulation of these ion co-transporters, and hence electrolyte balance, is the WNK-SPAK/OSR1 signaling pathway.[2] The first link between this signaling pathway and electrolyte balance was noted when mutations in the genes encoding the serine/threonine protein with no lysine (K) (WNK) kinases resulted in an inherited form of hypertension in humans known as Gordon's syndrome.[3] Subsequent studies identified two serine/threonine protein kinases, namely the STE20/SPS1-related proline/alanine-rich kinase (SPAK) and the oxidative-stress-responsive kinase 1 (OSR1), as the physiological substrates of WNK kinases (Figure 1a).[4] These two kinases were found to be able to phosphorylate a series of sodium, potassium and chloride ion co-transporters such as the Na-K-Cl co-transporters 1 and 2 (NKCC1 and 2), the Na-Cl co-transporter (NCC) and the K-Cl co-transporter (KCC) (Figure 1a).[5] Various WNK, SPAK and OSR1 mouse models indicated that the inhibition of these kinases resulted in a lowered blood pressure through reduced in vivo phosphorylation of ion co-transporters.[6] These highlighted the WNK-SPAK/OSR1 signaling pathway as a plausible target in the discovery of new antihypertensive agents.

Human SPAK and OSR1 protein kinases are 68% identical in sequence and share a 92-amino acids highly conserved carboxy-

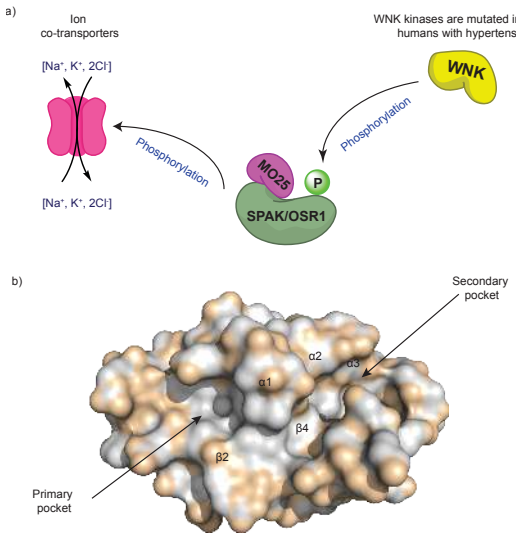

Figure 1. a) A brief depiction of WNK-SPAK/OSR1 signaling. b) Crystal structure of the human OSR1 CCT domain (452-end) showing the key primary and secondary pockets.

terminal (CCT) domain (aa. 436-527 for OSR1 and 456-547 for SPAK), which is 79% identical in sequence.[7] The CCT domain, which is highly conserved in orthologues of SPAK and OSR1 kinases in Caenorhabditis elegans, Drosophila and Xenopus,[8] binds RFxV (Arg-Phe-Xaa-Val) motifs of the upstream and downstream protein partners.[5c, 7, 9] The crystal structure of OSR1 CCT domain in complex with an 18-mer RFQV peptide derived from the upstream kinase WNK4 identified a *C*-terminal site, termed the primary pocket, as being responsible for mediating the binding to the upstream WNK kinases and downstream protein binders, *i.e.* ion co-transporters (Figure 1b).[8] Notably, a highly conserved second pocket, termed the secondary pocket, formed by a large loop connecting α3 to β4 was also observed (Figure 1b),[8] but the function of this site remained elusive. Intrigued by this, we sought to understand whether this secondary pocket had an impact on the catalytic activity of SPAK and OSR1 kinases and whether it is amenable to targeting by small molecules.

Initially, we explored the effect of the secondary pocket on catalytic activity of OSR1. To do this, we mutated the secondary pocket L440, S443 and V507 amino acid residues of OSR1. These three mutations were introduced to OSR1 T185E, where threonine 185 was mutated into glutamic acid to mimic WNK phosphorylation at this site, making the kinase constitutively active in vitro.[4] GST-tagged full length OSR1 T185E with single point mutations in the CCT domain was overexpressed and purified from HEK293. The catalytic activity of these kinases was established using Promega's luminescence ADP-Glo™ kinase assay.[10] As shown in Figure 2a, out of the three mutations studied, L440A and V507A showed significant in vitro reduction in the kinase activity of OSR1 T185E. Mutation of S443 into alanine, however, did not affect the kinase activity. To confirm that the L440A and V507A secondary pocket mutations, which influenced the kinase activity, have no effect on OSR1's CCT domain ability to bind WNK kinases, we used a fluorescence polarization assay

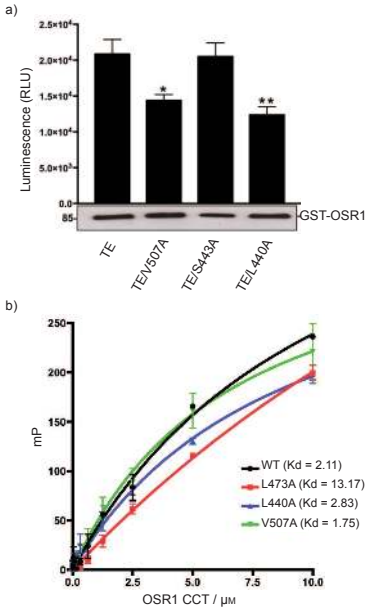

for measuring the binding of OSR1 CCT domain to an 18-mer RFQV peptide derived from the upstream kinase WNK.[6c] As a reference, we employed OSR1 CCT with a single point mutation L473A, which is located in the primary pocket and is known to reduce the binding of SPAK and OSR1 to WNK kinases.[11] The results revealed that the mutation in the primary pocket site, L473A, led to a significant reduction in binding to the WNK 18-mer RFQV peptide in agreement with the literature (CCT domain wild type Kd = 2.11 μM and CCT domain L473A Kd = 13.17 μM) (Figure 2b). Interestingly, the introduction of single point mutations in the secondary pocket did not affect the binding between OSR1 *C*-terminal domain and the WNK4 18-mer RFQV peptide (CCT domain L440A Kd = 1.83 μM and CCT domain V507V Kd = 1.75 μM) (Figure 2b). Together, this data represents the first evidence of the secondary pocket of OSR1 CCT domain being able to impact its kinase activity. Given the high similarity in sequence of the CCT domain of SPAK and OSR1, 79% sequence identity,[8] this site is very likely to influence the kinase activity of SPAK too.

Figure 2. Secondary pocket on OSR1 CCT domain affects its kinase activity. a) Single mutations in OSR1 T185E secondary pocket cause reduction in its kinase activity in vitro. *p <0.05 and **p <0.01. b) Fluorescence polarization analysis of the binding of OSR1 CCT wild-type (WT), primary pocket single point mutation (L473A), secondary pocket single point mutations (L440A and V507A) to an 18-mer RFQV peptide derived from WNK4. Data shown are the average signals with SD (*n* = 3).

Despite the compelling in vivo evidence of WNK-SPAK/OSR1 signaling inhibition yielding lowering in blood pressure,[6] there are currently no inhibitors of this signaling pathway in clinical development. However, numerous small molecules have been reported as potent inhibitors of WNK-SPAK/OSR1 signaling. These could be divided into two main groups; those which bind WNK kinases and the others which bind SPAK and OSR1. To date, only two compounds, WNK463[12] and compound 2[13], have been reported as WNK kinases inhibitors (structures not shown). However, few compounds that inhibit SPAK and OSR1 kinases directly without interfering with the kinase activity of WNKs have been described (Figure 3a).[14]

Encouraged by our observation of the secondary pocket playing a role in regulating OSR1 kinase activity, we subsequently conducted in silico docking of known WNK-signaling inhibitors that bind SPAK and OSR1 into the crystal structure of the human OSR1 CCT domain. For this we used AutoDock[15] and docked STOCK1S-50699,[14b] STOCK2S-26016,[14b] STOCK1S-14279[14a] and Closantel[14a] (Figure 3a), which are all WNK-SPAK/OSR1 signaling inhibitors, unbiasedly into the crystal structure of the reported OSR1 CCT domain. All of the docking possibilities placed Closantel and STOCK1S-50699 as well as the other reported small molecule WNK-signaling inhibitors in the secondary pocket (Figure 3b and supplementary Figures S1-3). Notably, a similar exercise using the RFQV tetrapeptide, which is known to bind the primary pocket[8] resulted in the docking of this tetrapeptide only in the primary pocket as expected (Figure 3b and supplementary Figures S4).

Subsequently, we focused our efforts into studying Closantel and STOCK1S-50699. Since OSR1 T185E exhibits superior in vitro kinase activity to SPAK T233E,[16] we focused our work on OSR1 T185E. In vitro kinase assays confirmed the ability of STOCK1S-50699 and Closantel to inhibit OSR1 T185E in vitro, IC_{50} = 40.26 μM and 8.65 μM and respectively (Figure 3c and 3e). The in vitro inhibition potency of STOCK1S-50699 (IC_{50} = 40.26 μM) is comparable to that reported[14b] in the initial discovery of STOCK1S-50699 (IC_{50} = 30-37 μM) though different kinase assays were used. The inability of Closantel and STOCK1S-50699 to inhibit the constitutively active truncated version of OSR1 T185E 1-342 (Figure 3d, 3f and supplementary Tables S1-2), which lacks the CCT domain and the secondary pocket, indicated that these inhibitors produce their action by binding to the CCT domain. Critically, these compounds were found to inhibit OSR1 T185E in vitro in an ATP-independent manner in

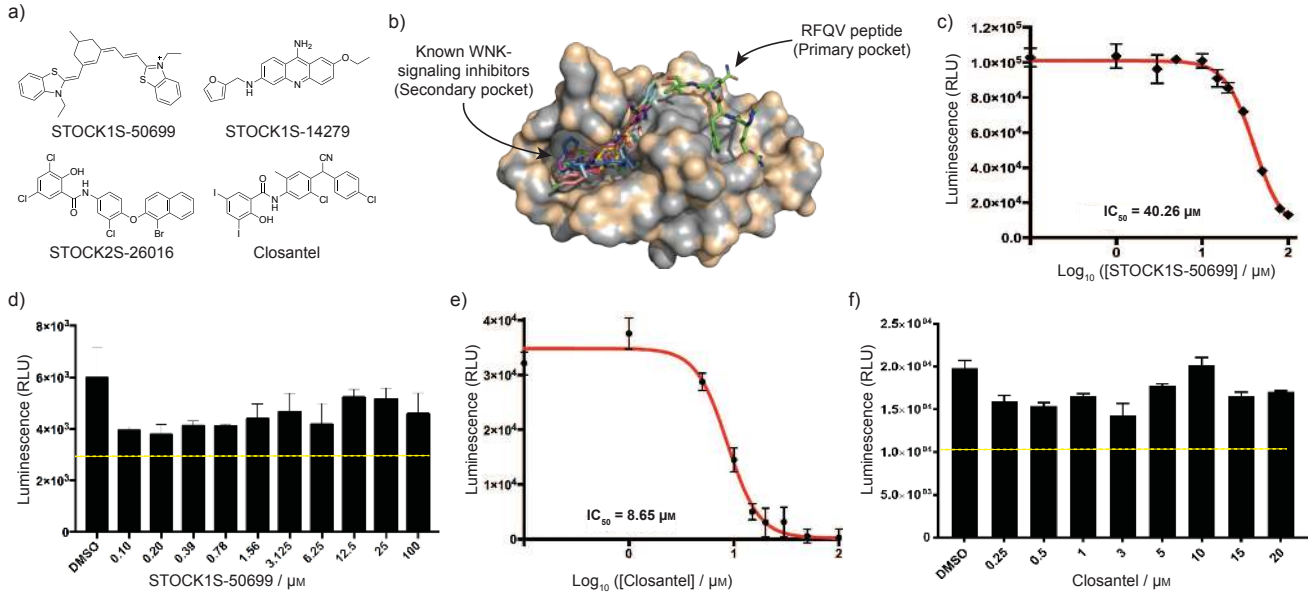

Figure 3. Known WNK-SPAK/OSR1 signaling inhibitors bind to OSR1 CCT domain secondary pocket. a) Chemical structures of the WNK-SPAK/OSR1 signaling inhibitors used in the in silico docking studies. b) AutoDock results of the four WNK-SPAK/OSR1 signaling inhibitors showing exclusive binding to the secondary pocket of OSR1 CCT domain. The tetrapeptide RFQV (green sticks) binds to the primary pocket of OSR1 CCT domain. ADP-Glo™ in vitro kinase assay of STOCK1S-50699 c) and Closantel e) showing inhibition of OSR1 T185E. ADP-Glo™ in vitro kinase assay of STOCK1S-50699 d) and Closantel f) showing that they do not inhibit truncated OSR1 T185E 1-342, which lacks the C-terminal domain. Data shown in c), d), e) and f) are the average signals with SD (*n* = 3). The dotted yellow lines in d) and f) indicate 50% of the maximum kinase activity.

agreement with previous observations (supplementary Figure S5).[14] These results explain the mechanism by which Closantel inhibits OSR1 T185E as it was first reported as a non-ATP competitive inhibitor of SPAK and OSR1, but the binding site was unknown.[14a] As for STOCK1S-50699, our data showed that it inhibits constitutively active OSR1 T185E in vitro in assay conditions that lack the upstream kinase WNK4. This was surprising since STOCK1S-50699 was discovered as in inhibitor of SPAK and OSR1 binding to WNK kinases.[14b] This suggests that STOCK1S-50699 may have a dual mechanism of action that involves the inhibition of active OSR1 T185E by binding to the secondary pocket of the *C*-terminal domain as well as preventing its binding to upstream kinases. Critically, this dual mechanism of action may explain the higher potency of STOCK1S-50699 in cells, where it completely inhibits the phosphorylation of the ion co-transporters at a concentration nearly 3-fold lower than its in vitro IC_{50}.[5a, 14b]

To further test our finding of the secondary pocket of the CCT domain playing a role in regulating the kinase activity of OSR1, we next performed in silico screening of a 1,200 compounds FDA-approved compounds aimed at identifying novel small molecules that bind the secondary pocket of OSR1 CCT domain. Among the top hits identified was Rafoxanide (Figure 4a), a potent anti-parasitic agent[17] that is used to control infestations in animals. This compound stood out because of its structurally similarity to Closantel as they both share a 2-hydroxy-*N*-phenylbenzamide core. In vitro kinase assays using Rafoxanide showed it to be a low micromolar inhibitor of OSR1 T185E in vitro, IC_{50} = 8.18 μM (Figure 4b). Akin to Closantel and STOCK-1S-50699, Rafoxanide's in vitro inhibition of OSR1 T185E was a result of binding to the CCT domain since it did not show any significant inhibition of active OSR1 T185E 1-342, which lacks the *C*-terminal domain (Figure 4c, supplementary Figure S6 and Table S3). Additionally, ATP-competition assay showed that Rafoxanide is not an ATP-competitive inhibitor of full length active OSR1 T185E (Figure 4d and supplementary Figure S7).

Encouraged by Rafoxanide's ability to inhibit OSR1 T185E in vitro, we explored its ability to inhibit SPAK T233E in vitro. In order to improve SPAK T233E's in vitro activity, we run an in vitro kinase in the presence of the scaffolding protein MO25, which is known to enhance the in vitro activity of SPAK T233E by 80-fold.[16] The results indicated that Rofoxanide was also a low micromolar inhibitor of SPAK T233E in vitro (IC_{50} = 13.03 μM) (supplementary Figure S8). Notably, Rafoxanide was able to inhibit OSR1 T185E in vitro in the presence of MO25 with a similar potency (IC_{50} = 13.91 μM) (supplementary Figure S8).

Next, we studied Rafoxanide's ability to inhibit SPAK and OSR1 in cells. As shown in Figure 4e, treatment of HEK293 cells with hypotonic buffer[18] led to a significant increase in the phosphorylation of endogenous NKCC1 at residues T203, T207 and T212, which are SPAK and OSR1 phosphorylation sites. Additionally, SPAK phosphorylation at S373 also increased following hypotonic treatment indicating the activation of WNK kinases. The addition of 10 μM STOCK1S-50699 inhibited WNK-SPAK/OSR1 signaling as judged by lack of NKCC1 and SPAK S373 phosphorylation in agreement with previous reports.[5a] Interestingly, titration of Rafoxanide (1-50 μM) resulted in the inhibition of NKCC1 phosphorylation at residues T203, T207 and T212 indicating the inhibition of SPAK and OSR1 kinases similar to that observed with Closantel (Figure 4f). Total inhibition of these phosphorylation sites was observed at concentrations ≥ 20 μM. Notably, SPAK phosphorylation at S373 was not inhibited by Rafoxanide and Closantel, unlike with STOCK1S-50699, confirming the ability of these compounds to inhibit SPAK and OSR1 but not its ability to interact with WNK kinases, which phosphorylate SPAK S373.

In order to further establish that Rafoxanide binding to SPAK and OSR1 CCT domains does not take place in the primary pocket, we employed a biotin-streptavidin pulldown assay. For this, a biotinylated 18-mer RFQV peptide derived from human WNK4 was used to pulldown endogenous SPAK from HEK293 cell lysates.[8] As a negative control, we used the 18-mer AFQV peptide, which is known not to bind the primary pocket of SPAK

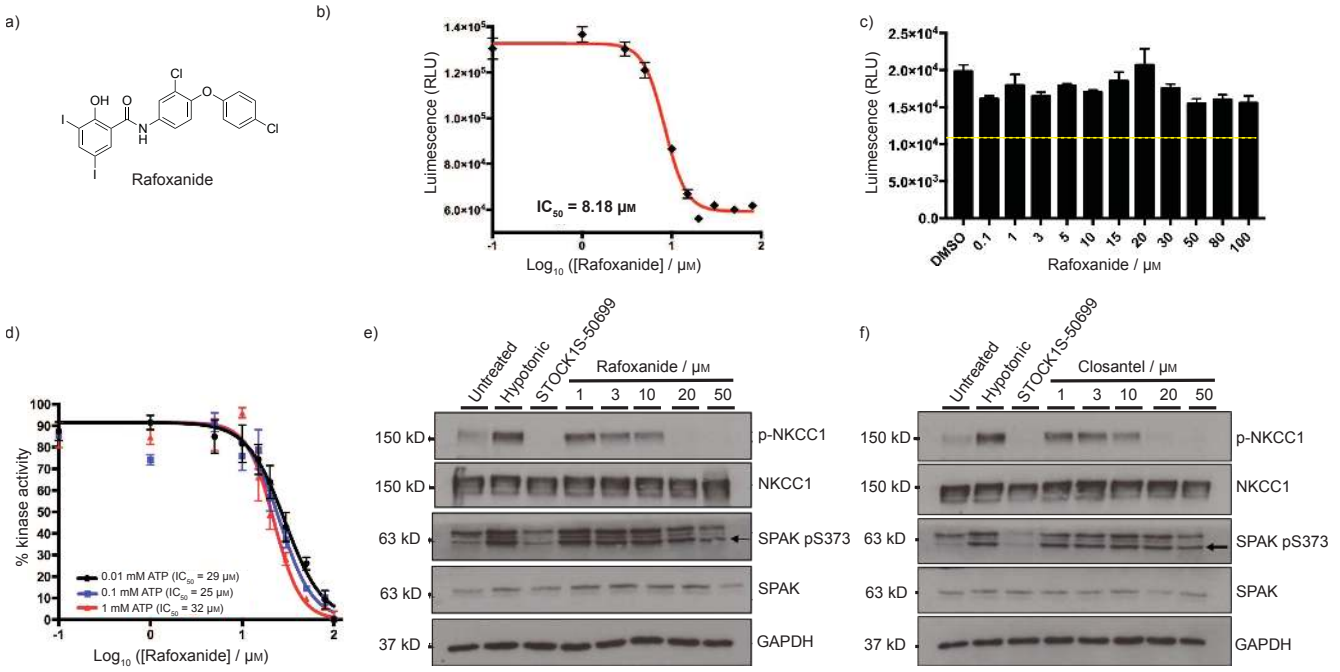

Figure 4. Rafoxanide is a novel allosteric inhibitor of SPAK/OSR1 in vitro and in cells. a) Chemical structure of Rafoxanide. b) Rafoxanide inhibits full length OSR1 T185E in vitro. The peptide CATCHtide was used as a substrate in the in vitro kinase assay. c) Rafoxanide does not inhibit the active truncated OSR1 T185E 1-342 in vitro. d) Rafoxanide inhibits OSR1 T185E in an ATP-independent manner. NKCC1 (1-174) was used as a substrate in the in vitro kinase assay. e) Rafoxanide and f) Closantel inhibit endogenous SPAK and OSR1 kinases in HEK293 cells. HEK293 cells were first treated with Rafoxanide (e) or Closantel (f) at the indicated concentrations or STOCK1S5 0699 (10 µM) for 30 min and then either left untreated or treated with hypotonic buffer for 30 min to activate WNK-SPAK/OSR1 signaling. The cells were then harvested, and the lysates were probed for phospho-NKCC1 T203, T207 and T212, total NKCC1, phospho-SPAKS373, total SPAK and GAPDH as a loading control. Data shown in b), c) and d) are the average signals with SD (*n* = 3). Data shown in e) and f) are representatives of three independent repeats. The dotted yellow line in c) indicates 50% of the maximum kinase activity.

and OSR1.[8] The pulldown was performed on cell lysates that either had been incubated with SPAK and OSR1 inhibitors, namely STOCK1S-50699, Closantel and Rafoxanide at the concentrations shown or left untreated (Figure 5a). The results showed that the 18-mer RFQV peptide was able to pull down endogenous SPAK while its mutant 18-mer AFQV peptide did not as expected.[8] Interestingly, Closantel and Rafoxanide did not compete with the 18-mer RFQV peptide, which binds to the primary pocket, even at high concentration (up to the 300 µM used) (Figure 5a). STOCK1S-50699 also failed to efficiently compete with the 18-mer RFQV peptide binding to SPAK except at high concentrations, 300 µM. Additionally, we carried out an FP assay for measuring the binding affinity of the 18-mer RFQV peptide derived from WNK4 to OSR1 CCT wild-type in presence of three different concentrations of Rafoxanide (1, 10 and 100 µM). The results showed that Rafoxanide was not able to compete with the RFQV peptide for binding to the primary pocket of OSR1 CCT wild-type even at 100 µM (Figure 5b). Collectively, the data shown in Figure 5 suggest that Rafoxanide and Closantel do not affect the 18-mer RFQV binding to OSR1 CCT domain primary pocket.

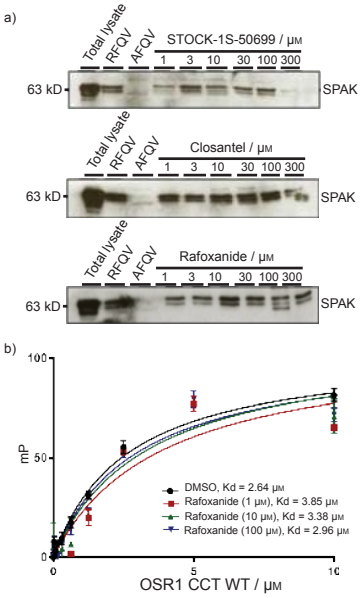

Figure 5. Rafoxanide and Closantel do not compete with the 18-mer RFQV peptide for binding to the primary pocket. a) Biotinylated 18-mer RFQV peptide was used to pull-down endogenous SPAK from HEK293 cells in the absence or presence of the inhibitors at the indicated concentrations. The biotinylated 18-mer AFQV peptide was used as a negative control. The data shown is representative of three independent repeats. b) Fluorescence polarization analysis of the binding of OSR1 CCT wild-type (WT) to the 18-mer RFQV peptide derived from WNK4 in the absence (DMSO) or presence of Rafoxanide at the indicated concentrations. Data shown are the average signals with SD (*n* = 3).

In conclusion, the highly conserved CCT domain secondary pocket of SPAK and OSR1 kinases plays an important role in regulating their kinase activity. This small pocket could be targeted by small molecules such as Closantel and Rafoxanide resulting in the inhibition of SPAK and OSR1 kinase activity in vitro. This finding will facilitate the rationale design of allosteric SPAK and OSR1 kinase inhibitors that could serve as powerful tools in the decoding of WNK-SPAK/OSR1 signaling. Importantly, allosteric SPAK and OSR1 kinase inhibitors may eventually be useful agents in treating hypertension and other diseases with sodium, potassium and chloride (electrolyte) imbalances.

Experimental Section

Reagents

Rafoxanide, Closantel, tissue-culture reagents and protein expression materials were purchased from Sigma Aldrich. STOCK1S-50699 was purchased from Vitas-M Laboratory, Ltd while glutathione–sepharose beads were purchased from GE Healthcare. Peptides were purchased from GLS Peptide Synthesis (China). ADP-Glo™ Kinase Assay kit was purchased from Promega. Lumio Green (FlAsH-EDT$_2$) was purchased from Carbosynth.

Buffers

Cells Lysis Buffer: 50 mM Tris-HCl (pH 7.5), 1 mM EDTA, 1 mM EGTA, 50 mM sodium fluoride, 5 mM sodium pyrophosphate, 1 mM sodium orthovanadate, 1% (w/v) Nonidet P40, 0.27 M sucrose, 0.1% (v/v) 2-mercaptoethanol, 0.1 mM PMSF, 1 mM benzamidine. Bacterial lysis buffer: 50 mM Tris-HCl (pH 7.5), 150 mM NaCl, 1 mM EGTA, 1 mM EDTA, 0.27 M sucrose, 0.1 mM PMSF, 1 mM benzamidine, 0.5 mg/ml lysosome, 0.3 mg/ml DNase and 0.01% (v/v) 2-mercaptoethanol. Buffer A: 50 mM Tris-HCl (pH 7.5), 0.1 mM EGTA and 0.1% (v/v) 2-mercaptoethanol. Normal buffer: bacterial lysis buffer without lysozome and DNase. High salt buffer: normal buffer with 500 mM NaCl. Protein elution buffer: buffer A and 20 mM reduced glutathione (pH 8). TBS-T buffer: 50 mM Tris-HCl (pH 7.5), 150 mM NaCl and 0.2% (v/v) Tween-20. Running buffer: 34.6 mM SDS, 25 mM Tris-base and 1.92 M glycine. Transfer buffer: 48 mM Tris-base, 39 mM glycine containing 20% (v/v) Methanol. Hypotonic low-chloride buffer: 67.5 mM sodium gluconate, 2.5 mM potassium gluconate, 0.25 mM $CaCl_2$, 0.25 mM $MgCl_2$, 0.5 mM Na_2HPO_4, 0.5 mM Na_2SO_4 and 7.5 mM HEPES. SDS sample buffer (4X): 40 % glycerol, 240 mM Tris-HCl (pH 6.8), 8% SDS, 0.04% bromophenol blue and 5% 2-mercaptoethanol. Blocking buffer: 10% (w/v) dried skimmed milk in TBST. Dialysis buffer: 50 mM Tris-HCl (pH 7.5), 150 mM NaCl and 2 mM dithiothreitol (DTT).

Antibodies

SPAK phospho-Ser373 antibody (residues 367–379) of human SPAK phosphorylated at Ser373 [S670B], NKCC1 total-antibody (residues 1-260) of shark NKCC1 [DU 6146], NKCC1 phospho-Thr 203+Thr 207+Thr 212 antibody (residues 198-217) of human NKCC1 phosphorylated at Thr 203 +Thr 207 +Thr 212 [S763B] and SPAK total-antibody (full length) of human SPAK [S551D] were purchased from Division of Signal Transduction Therapy Unit (University of Dundee). SPAK total-antibody [2281S] were from Cell Signaling Technology, GAPDH antibody [MA5-15738], Horseradish peroxidase (HRP)-labelled GST-total antibody [MA4-004-HRP], anti-sheep [31480] and anti-rabbit [31460] secondary antibodies conjugated to HRP were purchased from Thermo Scientific.

Plasmids, protein expression and purification

DNA clones were purchased from the Division of Signal Transduction Therapy (University of Dundee); pGEX-6P-1-OSR1 (433-end) [DU10096], pGEX-6P-1-OSR1 (433-end) L440A [DU 10332], pGEX-6P-1-OSR1 (433-end) V507A [DU 10331], pGEX-6P-1-OSR1 (433-end) S443A [DU 10330] and pGEX-6P-1-OSR1 (433 – end) L473A [DU 10321]. The proteins were expressed in *E. Coli* and purified as described elsewhere[16].

Cell culture and transfection

Human embryonic kidney 293 (HEK-293) cells were cultured on either 6-well plates or 10-cm dishes in Dulbecco's modified Eagle's medium (DMEM) supplemented with 10% (v/v) fetal bovine serum, 2 mM L-glutamine, 100 units/ml penicillin and 0.1 mg/ml streptomycin at 37 °C in a humidified 5% CO_2 incubator. For transfection, OSR1 T185E was transfected into cells using 20 µl of 1 mg/ml polyethylenimine (Polysciences) and 3 µg of plasmid DNA [19]. After 36 h transfection, cells were lysed in 0.4 ml of ice-cold lysis buffer. The lysates were clarified by centrifugation at 4 °C for 15 min at 26,000 *g* and the supernatants were stored at −80 °C. For inhibition studies, cells were incubated with each compound at indicated concentrations for 40 minutes then stimulated with low chloride hypotonic buffer to activate WNK signaling for 30 minutes. Then cells were lysed with 0.15 mL ice cold cells lysis buffer and centrifuged at 12000 *g* at 4 ºC for 10 minutes to collect the protein. The final DMSO concentration was < 0.1%.

Immunoblotting

Twenty µg of cell lysates, 0.2–1 µg of purified proteins or immunoprecipitates in SDS sample buffer were subjected to electrophoresis on a polyacrylamide gel and transferred to nitrocellulose membranes. The membranes were incubated for 1 h with TBS-T containing either 10% (w/v) skimmed milk powder (for antibodies raised in sheep) or 5% (w/v) BSA (for all other antibodies). The membranes were then immunoblotted in the same buffer for 1 h at room temperature with the indicated primary antibodies. Sheep antibodies were used at a concentration of 0.5–1 µg/ml, whereas commercial antibodies were diluted to 1000-fold. The incubation with phosphospecific sheep antibodies was performed with the addition of 10 µg/ml of the dephosphopeptide antigen used to raise the antibody. The blots were then washed six times with TTBS and incubated with secondary HRP-conjugated antibodies in 5% skimmed milk. After repeating the washing steps, the signal was detected with the enhanced chemiluminescence reagent. Immunoblots were developed using a film automatic processor (SRX-101; Konica Minolta Medical), and films were scanned with a 300-dp1 resolution on a scanner (PowerLook 1000; UMAX).

ADP-Glo™ in vitro kinase assay

350 µg of HEK293 lysates overexpressing GST-tagged full-length OSR1 T185E, wild-type or with secondary pocket mutations was incubated with 10 µL of sepharose-beads at 4 ºC. After 1 hour, the suspension was centrifuged at 3000 *g* at 4 ºC for 2 minutes. The beads then washed two times with cold lysis buffer containing 0.5 M NaCl and two times with buffer A. 10 µl aliquot of the kinase loaded sepharose beads was used in an in vitro kinase assay employing 0.25 mM CATCHtide (RRHYYYDTHTNTYY LRTFGHN TRR)[7]. Kinase reactions were performed for 40 minutes at 30 °C with gentle agitation in 25 µl reaction buffer consisting of 50 mM Tris-HCl, 10 mM $MgCl_2$, 0.1% (v/v) 2-mercaptoethanol, 0.1 mM ATP. The mixture was then transferred to a 96 well plate and developed using the Promega's ADP-Glo™ kit instructions[10] and the plate was subsequently read on a BMG FLUOstar Omega plate reader. For testing kinase assays that determined the IC_{50} values of the inhibitors, the kinase assay was performed in 384 well plates by incubating increasing concentration of inhibitors with GST-OSR1 T185E purified from *E.Coli* at 5 µL total reaction volume. The kinase activity was assayed using ADP-Glo™ kinase assay according to the manufacturer's protocol[10]. The plate was subsequently read on a BMG FLUOstar Omega plate reader. The final DMSO concentration was < 4%. Each sample was run in triplicate and the experiment was run three independent times. Data presented in figures is the average signal with SD (n = 3).

Fluorescence Polarization Assay (FP)

The RFQV peptide (CCPGCCGGSEEGKPQLVGRFQVTSSK) powder was initially resuspended in 50 mM NH_4HCO_3 (pH 8). Subsequently, it was labeled with FlAsH-EDT$_2$ fluorophore that binds covalently to the CCPGCC *N*-terminal motif on the RFQV peptide. The labeling step was achieved by incubating 10 µM of peptide with 30 µM of FlAsH-EDT$_2$ in 500 µl dialysis buffer in the dark at 4 °C for 2 h. The peptides were then dialyzed for 4 h into dialysis buffer using a Mini Dialysis kit with 1 kD cut-off (GE Healthcare) and then for another 12 h with a fresh dialysis buffer. The optimum FlAsH-EDT$_2$ concentration that exhibited about ten times more fluorescence intensity signal compared to background controls was 10 nM. For the fluorescence polarization studies, 10 nM of FlAsH-EDT$_2$ labelled peptide was mixed with proteins at various concentrations (0.005-5 µM) in dialysis buffer in a final volume of 30 µL. Each assay was performed in triplicate with at least twelve data points per curve and repeated three independent times. A BMG PheraStar plate reader was used to measure the fluorescence polarization, with an excitation and emission wavelengths of 485 nm and 538 nm, respectively.[11] Data presented in figures is the average signal with SD (n = 3).

AutoDock docking

Autodock Vina 1.1.2[20] was used to dock the current available WNK signaling inhibitors against the crystal structure of OSR1 CCT (PDB ID: 2V3S). AutoDock tool 1.5.6[21] was used for preparation of pdbqt files of proteins and ligands. The unbiased docking approach was initially optimized in term of docking exhaustiveness and subsequently validated

by re-docking WNK4-RFQV into OSR1 CCT (PDB ID: 2V3S) and PP1 into Hck ATP site (PDB ID:1QCF). The same approach was used to perform structure-based virtual screening (SBVS) of 1200 FDA-approved compounds using PyRx virtual screening tool. The docking results were visualized and analyzed using Discovery Studio 4.5 (Accelrys, San Diego, CA) and PyMOL Molecular Graphics System 1.3.

Biotin-streptavidin pulldown assay

250 µg of pre-cleared HEK-293 total cells lysates were incubated with inhibitors at the indicated concentrations for 2 h at 4 ºC. 3 µg of biotinylated 18-mer RFQV-containing peptide derived from WNK4 (biotin-SEEGKPQLVGRFQVTSSK) or the 18-mer AFQV-containing peptide (biotin-SEEGKPQLVGAFQVTSSK) were added and incubated under the same condition for a further 15 minutes at 4 ºC. Then, to each sample 20 µl of streptavidin beads equilibrated in cells lysis buffer (pre-washed 3X with phosphate-buffered saline) was added and incubated for 15 minutes at 4 ºC. After the incubation, the beads were washed two times with cell lysis buffer and twice with Buffer A, respectively. Then, they were boiled with 1XSDS sample buffer and subjected to SDS-PAGE. The data shown is a representative of three independent repeats.

Acknowledgements

We would like to thank the MRC for funding parts of this project through an MRC Confidence of Concept Grant (reference MC_PC_14107). We are also grateful to the Birmingham Protein Expression Facility (PEF) for help with protein production. MAA is funded by a PhD studentship from the Ministry of Education in Saudi Arabia and Prince Sattam Bin Abdulaziz University. NSS would like to thank the Royal Society for the award of an Industry Fellowship.

Keywords: SPAK • OSR1 • Kinase • Inhibitor • Allosteric

References:

[1] aG. Gamba, *Physiol Rev* **2005**, *85*(2), 423-493; bK. Kaila, T. J. Price, J. A. Payne, M. Puskarjov, J. Voipio, *Nat Rev Neurosci* **2014**, *15*(10), 637-654; cS. N. Orlov, S. V. Koltsova, L. V. Kapilevich, S. V. Gusakova, N. O. Dulin, *Genes Dis* **2015**, *2*(2), 186-196.

[2] aD. R. Alessi, J. Zhang, A. Khanna, T. Hochdorfer, Y. Shang, K. T. Kahle, *Sci Signal* **2014**, *7*(334), re3; bJ. Hadchouel, D. H. Ellison, G. Gamba, *Annu Rev Physiol* **2016**, *78*, 367-389.

[3] F. H. Wilson, S. Disse-Nicodeme, K. A. Choate, K. Ishikawa, C. Nelson-Williams, I. Desitter, M. Gunel, D. V. Milford, G. W. Lipkin, J. M. Achard, M. P. Feely, B. Dussol, Y. Berland, R. J. Unwin, H. Mayan, D. B. Simon, Z. Farfel, X. Jeunemaitre, R. P. Lifton, *Science* **2001**, *293*(5532), 1107-1112.

[4] A. C. Vitari, M. Deak, N. A. Morrice, D. R. Alessi, *Biochem J* **2005**, *391*(Pt 1), 17-24.

[5] aP. de Los Heros, D. R. Alessi, R. Gourlay, D. G. Campbell, M. Deak, T. J. Macartney, K. T. Kahle, J. Zhang, *Biochem J* **2014**, *458*(3), 559-573; bZ. Melo, P. de los Heros, S. Cruz-Rangel, N. Vazquez, N. A. Bobadilla, H. Pasantes-Morales, D. R. Alessi, A. Mercado, G. Gamba, *J. Biol. Chem.* **2013**, *288*(44), 31468-31476; cT. Moriguchi, S. Urushiyama, N. Hisamoto, S. Iemura, S. Uchida, T. Natsume, K. Matsumoto, H. Shibuya, *J Biol Chem* **2005**, *280*(52), 42685-42693; dJ. Ponce-Coria, P. San-Cristobal, K. T. Kahle, N. Vazquez, D. Pacheco-Alvarez, P. de Los Heros, P. Juarez, E. Munoz, G. Michel, N. A. Bobadilla, I. Gimenez, R. P. Lifton, S. C. Hebert, G. Gamba, *Proc Natl Acad Sci U S A* **2008**, *105*(24), 8458-8463; eC. Richardson, F. H. Rafiqi, H. K. Karlsson, N. Moleleki, A. Vandewalle, D. G. Campbell, N. A. Morrice, D. R. Alessi, *J. Cell Sci.* **2008**, *121*(Pt 5), 675-684.

[6] aF. H. Rafiqi, A. M. Zuber, M. Glover, C. Richardson, S. Fleming, S. Jovanovic, A. Jovanovic, K. M. O'Shaughnessy, D. R. Alessi, *EMBO Mol Med* **2010**, *2*(2), 63-75; bS. S. Yang, Y. F. Lo, C. C. Wu, S. W. Lin, C. J. Yeh, P. Chu, H. K. Sytwu, S. Uchida, S. Sasaki, S. H. Lin, *J Am Soc Nephrol* **2010**, *21*(11), 1868-1877; cJ. Zhang, K. Siew, T. Macartney, K. M. O'Shaughnessy, D. R. Alessi, *Hum Mol Genet* **2015**.

[7] A. C. Vitari, J. Thastrup, F. H. Rafiqi, M. Deak, N. A. Morrice, H. K. Karlsson, D. R. Alessi, *Biochem J* **2006**, *397*(1), 223-231.

[8] F. Villa, J. Goebel, F. H. Rafiqi, M. Deak, J. Thastrup, D. R. Alessi, D. M. van Aalten, *EMBO Rep* **2007**, *8*(9), 839-845.

[9] aA. N. Anselmo, S. Earnest, W. Chen, Y. C. Juang, S. C. Kim, Y. Zhao, M. H. Cobb, *Proc Natl Acad Sci U S A* **2006**, *103*(29), 10883-10888; bK. B. Gagnon, R. England, E. Delpire, *Am J Physiol Cell Physiol* **2006**, *290*(1), C134-142; cK. Piechotta, N. Garbarini, R. England, E. Delpire, *J. Biol. Chem.* **2003**, *278*(52), 52848-52856.

[10] H. Zegzouti, M. Zdanovskaia, K. Hsiao, S. A. Goueli, *Assay Drug Dev Technol* **2009**, *7*(6), 560-572.

[11] J. Zhang, K. Siew, T. Macartney, K. M. O'Shaughnessy, D. R. Alessi, *Hum Mol Genet* **2015**, *24*(16), 4545-4558.

[12] K. Yamada, H. M. Park, D. F. Rigel, K. DiPetrillo, E. J. Whalen, A. Anisowicz, M. Beil, J. Berstler, C. E. Brocklehurst, D. A. Burdick, S. L. Caplan, M. P. Capparelli, G. Chen, W. Chen, B. Dale, L. Deng, F. Fu, N. Hamamatsu, K. Harasaki, T. Herr, P. Hoffmann, Q. Y. Hu, W. J. Huang, N. Idamakanti, H. Imase, Y. Iwaki, M. Jain, J. Jeyaseelan, M. Kato, V. K. Kaushik, D. Kohls, V. Kunjathoor, D. LaSala, J. Lee, J. Liu, Y. Luo, F. Ma, R. Mo, S. Mowbray, M. Mogi, F. Ossola, P. Pandey, S. J. Patel, S. Raghavan, B. Salem, Y. H. Shanado, G. M. Trakshel, G. Turner, H. Wakai, C. Wang, S. Weldon, J. B. Wielicki, X. Xie, L. Xu, Y. I. Yagi, K. Yasoshima, J. Yin, D. Yowe, J. H. Zhang, G. Zheng, L. Monovich, *Nat Chem Biol* **2016**, *12*(11), 896-898.

[13] K. Yamada, J. H. Zhang, X. Xie, J. Reinhardt, A. Q. Xie, D. LaSala, D. Kohls, D. Yowe, D. Burdick, H. Yoshisue, H. Wakai, I. Schmidt, J. Gunawan, K. Yasoshima, Q. K. Yue, M. Kato, M. Mogi, N. Idamakanti, N. Kreder, P. Drueckes, P. Pandey, T. Kawanami, W. Huang, Y. I. Yagi, Z. Deng, H. M. Park, *ACS Chem Biol* **2016**, *11*(12), 3338-3346.

[14] aE. Kikuchi, T. Mori, M. Zeniya, K. Isobe, M. Ishigami-Yuasa, S. Fujii, H. Kagechika, T. Ishihara, T. Mizushima, S. Sasaki, E. Sohara, T. Rai, S. Uchida, *J Am Soc Nephrol* **2015**, *26*(7), 1525-1536; bT. Mori, E. Kikuchi, Y. Watanabe, S. Fujii, M. Ishigami-Yuasa, H. Kagechika, E. Sohara, T. Rai, S. Sasaki, S. Uchida, *Biochem J* **2013**, *455*(3), 339-345.

[15] D. S. Goodsell, G. M. Morris, A. J. Olson, *J Mol Recognit* **1996**, *9*(1), 1-5.

[16] B. M. Filippi, P. de los Heros, Y. Mehellou, I. Navratilova, R. Gourlay, M. Deak, L. Plater, R. Toth, E. Zeqiraj, D. R. Alessi, *EMBO J* **2011**, *30*(9), 1730-1741.

[17] aS. E. Knapp, P. J. Presidente, *Am J Vet Res* **1971**, *32*(8), 1289-1291; bG. E. Swan, *J S Afr Vet Assoc* **1999**, *70*(2), 61-70.

[18] A. Zagorska, E. Pozo-Guisado, J. Boudeau, A. C. Vitari, F. H. Rafiqi, J. Thastrup, M. Deak, D. G. Campbell, N. A. Morrice, A. R. Prescott, D. R. Alessi, *J. Cell Biol.* **2007**, *176*(1), 89-100.

[19] Y. Durocher, S. Perret, A. Kamen, *Nucleic Acids Res.* **2002**, *30*(2), E9.

[20] O. Trott, A. J. Olson, *J. Comput. Chem.* **2010**, *31*(2), 455-461.

[21] M. F. Sanner, *J Mol Graph Model* **1999**, *17*(1), 57-61.

Entry for the Table of Contents

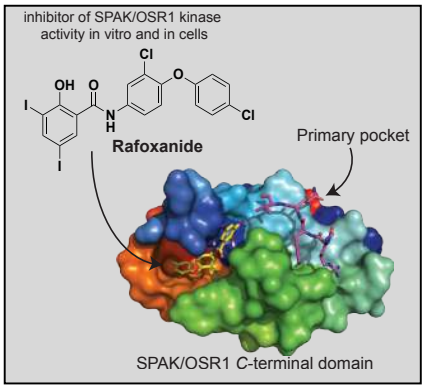

SPAK and OSR1 kinases regulate electrolyte balance in vivo. Herein, we identify a small pocket on their *C*-terminal domains that has a role in regulating their kinase activity. Using in silico screening, we discovered Rafoxanide as a novel allosteric inhibitor of these two protein kinases. Together, these findings will facilitate the discovery of allosteric SPAK and OSR1 inhibitors with potential antihypertensive effects.

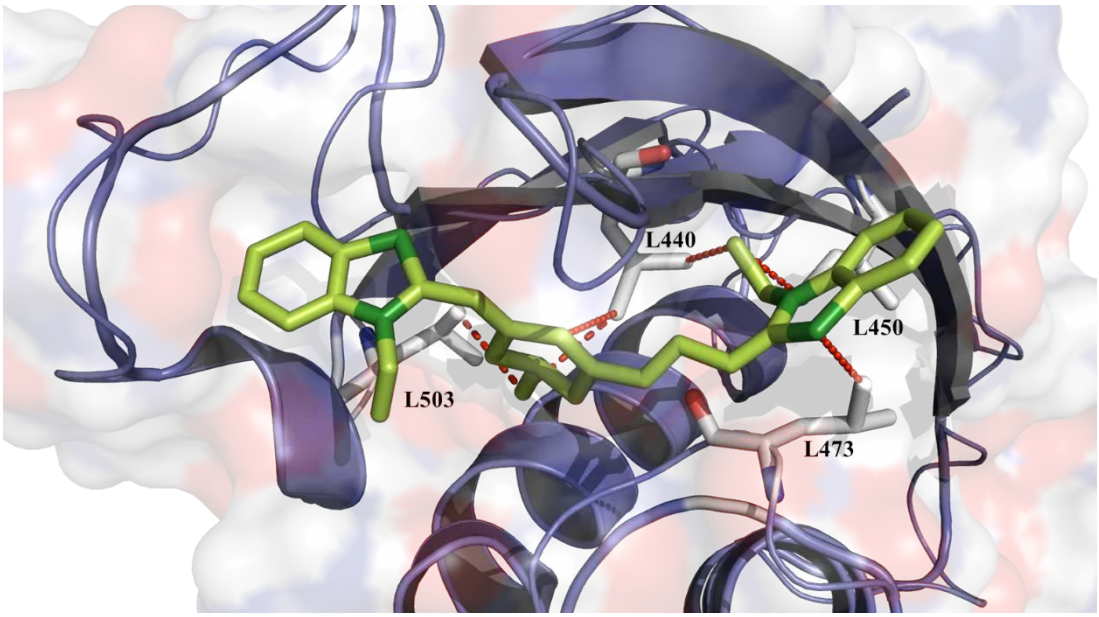

Supplementary figure S1. Docking of STOCK1S-50699 into OSR1 CCT domain using AutoDock Vina®.

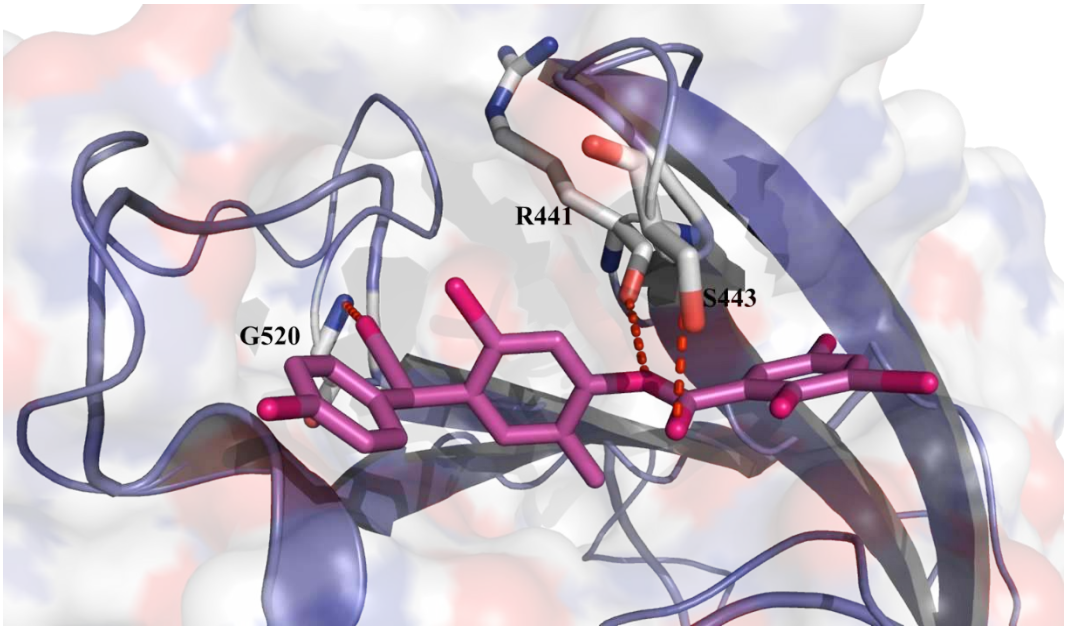

Supplementary figure S2. Docking of Closantel into OSR1 CCT domain using AutoDock Vina®.

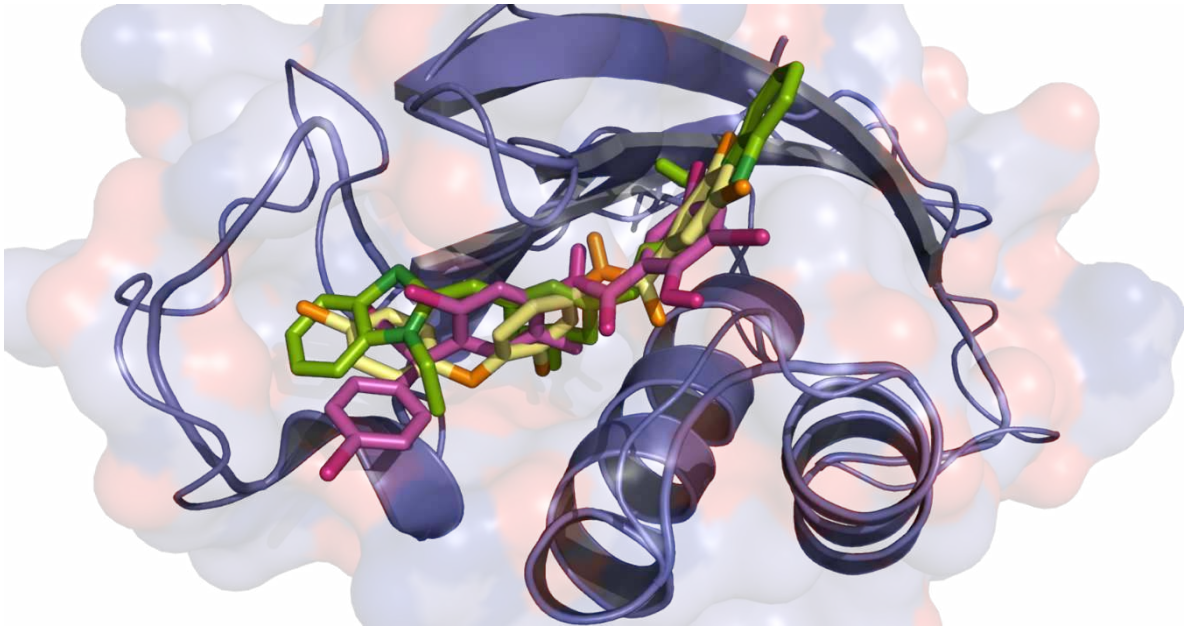

Supplementary figure S3. Docking of STOCK1S-50699 (green), Closantel (pink) and Rafoxanide (yellow) into OSR1 CCT domain using AutoDock Vina®.

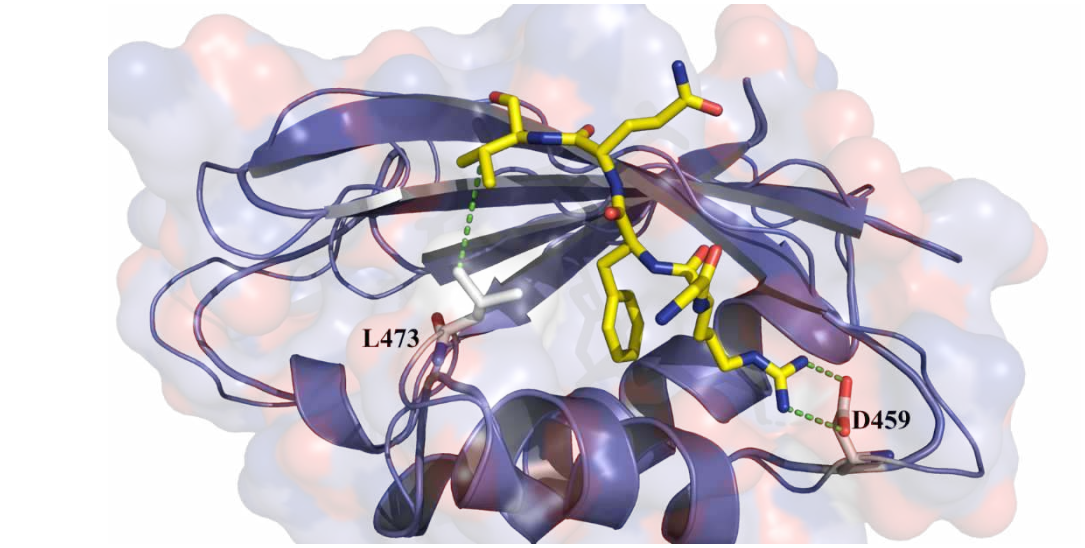

Supplementary figure S4. Docking of RFQV tetrapeptide into OSR1 CCT domain using AutoDock Vina®.

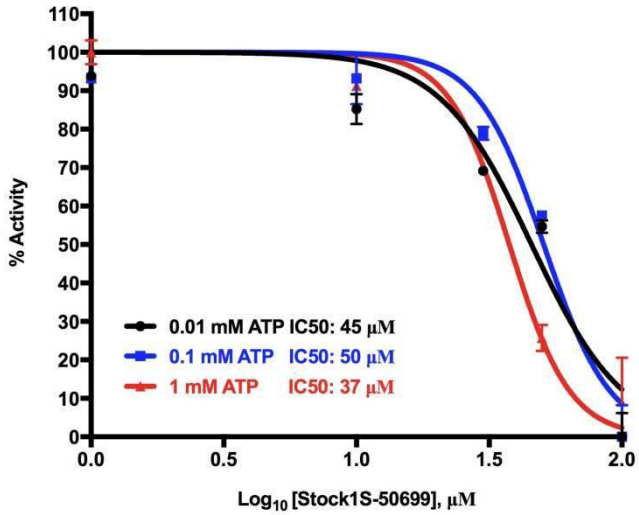

Supplementary figure S5. STOCK1S-50699 inhibits OSR1 T185E in vitro in an ATP-independent manner.

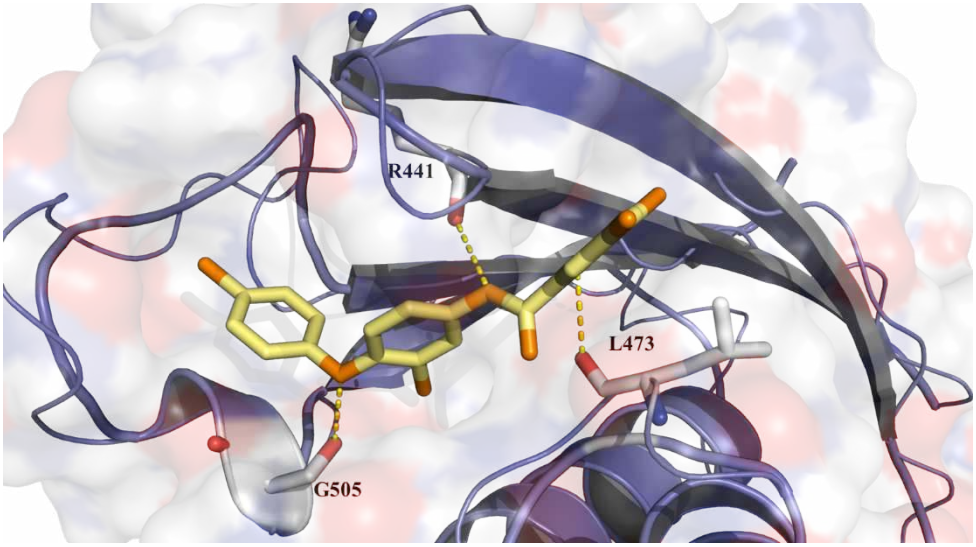

Supplementary figure S6. Docking of Rafoxanide in OSR1 CCT using AutoDock Vina®. OSR1 R441, L473 and S505 formed key hydrogen interactions with Rafoxanide.

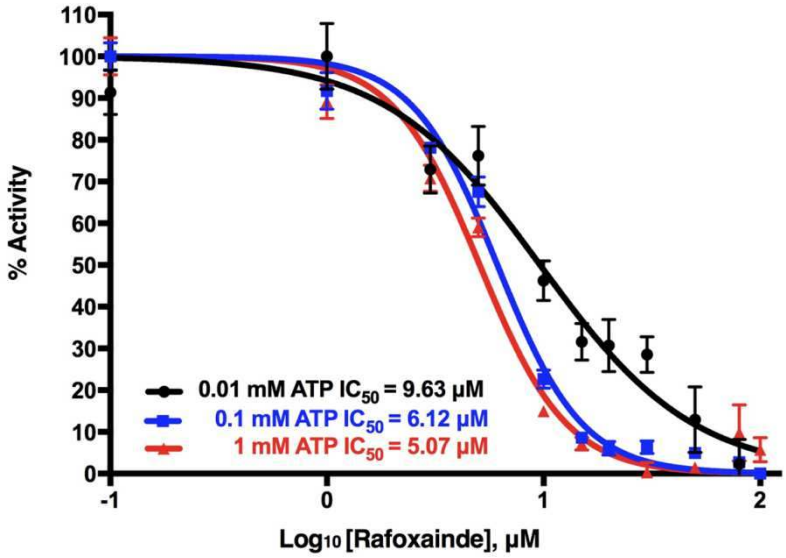

Supplementary figure S7. Rafoxanide inhibits OSR1 T185E in vitro in an ATP-independent manner. The peptide, CATCHtide, was used as a substrate in this assay.

a

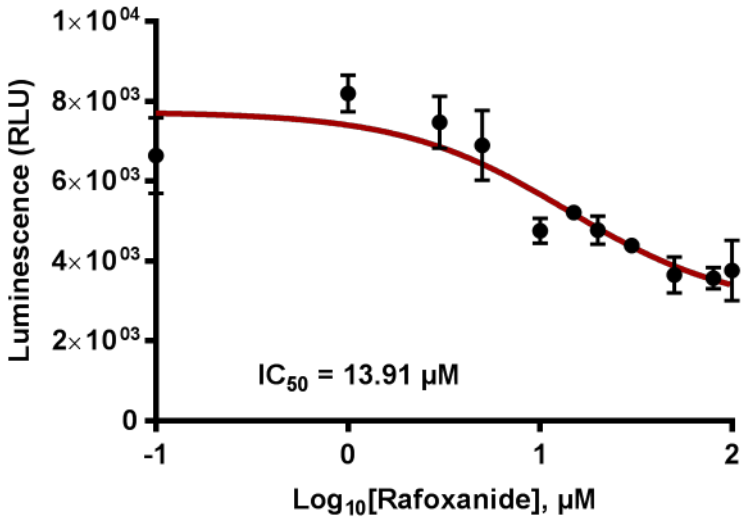

b

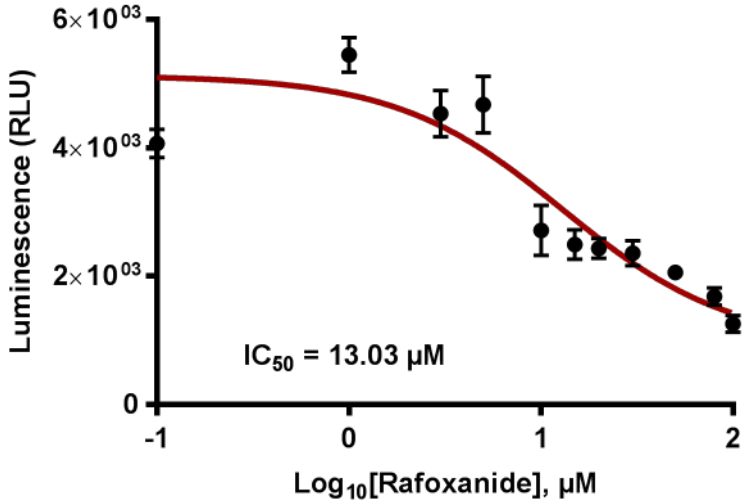

Supplementary figure S8. Rafoxanide inhibits both OSR1 TE (a) and SPAK TE (b) in vitro in the presence of MO25. The assay was performed in 384-well plate by incubating 1 µl of Rafoxanide at different concentrations with 0.2 µM GST-OSR1 T185E or 0.5 µM SPAK T233E in presence of 5 molar excess of MO25. The reaction was conducted in a 5 µl total reaction volume containing 50 mM Tris/HCl, 10 mM $MgCl_2$, 0.1% (v/v) 2-mercaptoethanol, 0.1 mM ATP employing 0.3 mM CATCHtide (RRHYYYDTHTNTYYLRTFGHNTRR) as substrate in buffer A at 30 °C for 30 min with gentle agitation. The kinase activity was assayed using ADP-Glo™ kinase assay according to the manufacturer's protocol. The plate was subsequently read on a BMG FLUOstar Omega plate reader. Data shown is the average of signals with SD (*n* = 3).

Concentration (µM)	Luminescence (RLU)	±SE
DMSO	5971.17	982.65
0.10	3933.67	134.72
0.20	3774.67	330.68
0.39	4116.67	153.50
0.78	4097.17	72.26
1.56	4384.67	476.02
3.125	4652.67	596.04
6.25	4168.67	673.61
12.5	5217.17	261.69
25	5147.67	360.07
100	4585.17	656.87

Table S1. In vitro ADP-Glo™ kinase assay raw data of OSR1 T185E 1-342 in presence of the indicated concentrations of STOCK1S-50699.

Concentration (µM)	Luminescence (RLU)	±SE
DMSO	19822.25	729.01
0.25	15989.50	397.80
0.5	15400.33	408.96
1	16605.00	263.72
3	14339.00	1354.28
5	17762.33	230.34
10	20208.33	885.13
15	16607.33	430.78
20	17118.33	74.96

Table S2. In vitro ADP-Glo™ kinase assay raw data of OSR1 T185E 1-342 in presence of the indicated concentrations of Closantel.

Concentration (μM)	Luminescence (RLU)	±SE
DMSO	19845.00	989.36
0.1	16143.00	459.92
1	17974.50	1664.57
3	16464.50	651.32
5	17871.50	343.93
10	17022.25	369.81
15	18573.75	1342.70
20	20690.67	2177.09
30	17572.25	622.16
50	15482.00	742.88
80	16050.00	712.93
100	15582.75	1104.13

Table S3. In vitro ADP-Glo™ kinase assay raw data of OSR1 T185E 1-342 in presence of the indicated concentrations of Closantel.